

The baseline wander correction based on improved EEMD algorithm for grounded electrical source airborne transient electromagnetic signals

Yuan Li¹, Song Gao^{2,3}, Saimin Zhang^{1,2}, Hu He³, Pengfei Xian³, Chunmei Yuan³

¹College of Geophysics, Chengdu University of Technology, Chengdu, 610059, China

²Key Laboratory of Earth Exploration and Information Techniques of Ministry of Education, Chengdu, 610059, China

³College of Information Science and Technology, Chengdu University of Technology, Chengdu, 610059, China

Correspondence to: Yuan Li (86210111@qq.com)

Abstract. The grounded electrical source airborne transient electromagnetic (GREATEM) system is an important method for obtaining subsurface conductivity distribution as well as outstanding detection efficiency and easy flight control. However, there are the superposition of desired signals and various noise for GREATEM signal. The baseline wander caused by the receiving coil motion always exists in the process of data acquisition to affect the measurement results. The baseline wander is one of the main noise sources which has its own characteristics such as the low frequency, large amplitude, non-periodic and non-stationary and so on. Consequently, it is important to correction GREATEM signal for inversion explanation. In this paper, we propose improving method of EEMD by adaptive filtering (EEMD-AF) based on ensemble empirical mode decomposition (EEMD) to suppress baseline wander. Firstly, the EEMD-AF method will decompose the electromagnetic signal into multi-stage intrinsic mode function (IMF) components. Subsequently, the adaptive filter will process higher index IMF components containing the baseline wander. Lastly, the de-noised signal will be reconstructed. To examine the performance of our introduced method, we processed the simulated and field signal containing the baseline wander by different methods. Through the evaluation of the signal-to-noise ratio (SNR) and mean-square-error (MSE), the result indicates that the signal using EEMD-AF method can get higher SNR and lower MSE. Comparing correctional data using the EEMD-AF and the wavelet-based method in the anomaly curves profile images of the response signal, it is proved that the EEMD-AF method is a practical and effective for the suppression of the baseline wander on GREATEM signal.

1 Introduction

The GREATEM system consists of two parts: the ground transmitter and air receiver system. This method takes advantage of the Airborne electromagnetic method (AEM) and the Magnetotelluric method (MT), which has large detection depth, higher signal resolution and outstanding detection efficiency (Mogi T, 1998; Smith R S, 2001).

There are the superposition of desired signals and various noise for GREATEM signal. The noise may be divided into stationary white noise and non-stationary noise. According to the various noise source, the noise is usually classified as sferics noise, human electromagnetic noise and motion-induced noise (Abderrezak et al.; 2010; Buselli et al.; 1998, Macnae et al., 1984). The sferics noise is mainly caused by the charge discharge in the atmosphere, and the frequency is within 1k Hz. Human electromagnetic noise is caused by 50 Hz or 60 Hz industrial frequencies and its odd harmonics. Motion-induced noise comes from the receiving coil motion and has its own characteristics, such as low frequency, large amplitude, non-periodic and non-stationary. The signal baseline wanders caused by motion noise is one of the major interferences with the GREATEM signal. This phenomenon always exists in the process of data acquisition to affect the measurement results. Severe baseline wander leads to inferior resistivity image formation and lower reliability of inversion explanation in the measured respond signal. After removing above noises, the processed data will be stacked and averaged on the next stage.

Because the receiver system is mounted on aircraft such as the rotor-wing unmanned aerial vehicle (UAV) and airship, GREATEM system is different from AEM. First, during the flight, because the vibration and speed of the aircraft are weaker than airborne electromagnetic system, the amplitude of the mounted coil swing is smaller. Hence, the fake anomalous amplitude of GREATEM caused by baseline wander is smaller than AEM. Second, there is narrower frequency distribution of baseline wander for GREATEM signal. The frequency distribution of the motion-induced noise is within 1k Hz for the AEM, while the frequency distribution of baseline is mostly within a few Hz for GREATEM in the actual measurement. Third, due to the use of miniaturized aircraft for GREATEM, the maximum flight loads are much less than the AEM. It is impossible to install the complex mechanical structure to suppress baseline wander on the receiver system. Therefore, it is necessary to develop the algorithm processing for the suppression of baseline wander.

In the method to suppress baseline wander, on the one hand the mechanical correctional structure and the hardware filter can be installed, on the other hand the digital filter and fitting can be used for data processing. Some of studies have focussed on the correctional method to suppress motion-induced noise on the transient electromagnetic system. The Fugro company developed the time domain airborne electromagnetic system where the hardware compensation devices and the notch filter with center frequency of 0.5 Hz are installed to correct coil motion in the data acquisition system. Buselli et al. (1998) proposed that the high-pass filter with a cut-off frequency of 10 Hz be used to reduce this noise. Lemire et al. (2001) raised the spline interpolation and Lagrange optimization method to reject low frequency noise. Yuan et al. (2013) introduced wavelet-based baseline drift correction method using sym8 wavelet and 10 decomposition layers. The wavelet-based method is based on multi-resolution decomposition analysis. But because it is difficult for wavelet decomposition to choose optimal wavelet basis function and layer levels, such methods have poor adaptability. Patrick et al. (2004) raised the detrend method based on EEMD. This method consists of two steps. First, the trend be regarded as baseline estimate which be expected to be captured by IMFs of large index. Second, the reconstructed signal be amounted to the partial IMFs from lower index to middle index without the higher index components directly. Fubo et al. (2017) focussed on EEMD method to distinguish and suppress motion-induced noise in grounded electrical source airborne TEM system. Because the components containing motion-induced noise are excluded from the reconstructed signal directly, the reconstructed signal was distorted by these EEMD method.

N.E.Huang et al. (1998) proposed the empirical mode decomposition (EMD) then Z. Wu et al.(2009) raised EEMD. The EMD and EEMD method is a scale-adaptive time-domain method which is applied to non-linear and non-stationary signal decomposition. For non-stationary signal processing, it is necessary to propose the short time Fourier transform (STFT) and wavelet transform generally. The main method of STFT is to divide the signal into short time intervals where the signal is approximately stationary, and then perform the Fourier transform of signal on each time interval to get the frequency distribution. And the main method of the wavelet transform is to utilize a variable-scale sliding window where the specific data is approximately stationary on signal. The width of window is variable for time and frequency domain. However, because it is difficult to choose optimal wavelet basis function and the layer levels of wavelet decomposition by the signal itself, this method has poor adaptability. Therefore, the requirement of signal characteristic above method is stationary in a specific window as same as the Fourier transform.

Different from previous methods, the major advantage of the EEMD is that the decomposition is derived from the signal itself. Therefore, the EEMD analysis is adaptive decomposition in contrast to the traditional methods that the decomposition functions are fixed in a specific window throughout the processing. In addition, the characteristics of the signal itself are not affected in the sifting process.

According to the characteristics of baseline wander for GREATEM signal, the EEMD-AF method consists of three steps.
step 1. The signal is decomposed into the N-level IMF components and the residual component by the EEMD method.
step 2. It is careful to use an adaptive low-pass filter for higher index IMFs to get baseline wander estimate.
step 3. The de-noised signal can be obtained by subtracting baseline wander from the noisy signal.

In the later sections, compared with that of wavelet-based and EEMD without the higher index components, the correctional result shows that the EEMD-AF method is a practical and effective for the suppression of the baseline wander on GREATEM signal.

2 Correctional method of EEMD-AF

2.1 EMD method

The signal $S(t)$ is decomposed into N-level IMF components and a residual component by the EMD method. The EMD involves the adaptive decomposition of signal $S(t)$ by means of the sifting process. The term of IMF is adopted because it represents the oscillation mode embedded in the data. The sifting process is defined by the following steps:

- step 1. Identify levels of decomposition N, and $r_{j-1}(t) = S(t)$ as residual parameter;
- step 2. Extract IMF_j;
 - (a) all extrema of $r_{j-1}(t)$;
 - (b) Interpolate local maxima and minima as the upper and lower envelopes separately by a cubic spline line. And compute 'envelope' $E_{\min}(t)$ and $E_{\max}(t)$;

(c) Compute the average component $m(t) = (E_{\min}(t) + E_{\max}(t))/2$;

95 (d) Extract the detail component $D_i(t) = x(t) - m(t)$;

(e) Iterate step (a) to step (d) on the detail component $D(t)$ until the stopping criterion satisfy threshold, $sd < \varepsilon$. Once criterion is achieved, the $D(t)$ is considered as the effective IMF_j which also be considered as zero-mean generally. Calculate stopping criterion:

$$sd = \sum \frac{|D_{i-1}(t) - D_i(t)|^2}{D_{i-1}(t)^2} \quad (1)$$

100 step 3. Update residual: $r_j(t) = r_{j-1}(t) - IMF_j(t)$, the residual is deemed as the input for a new round of iterations;

step 4. Repeat step 2 and 3 until the value of j equal to N .

The stop criterion threshold ε is set between 0.2 to 0.3. The result of the sifting procedure is that $S(t)$ will be decomposed into $IMF_j(t)$, $j = 1, \dots, N$ and residual $r_N(t)$.

$$S(t) = \sum_{j=1}^N IMF_j(t) + r_N(t) \quad (2)$$

105 2.2 EEMD method

The EEMD method is an improved method based on EMD method. Compared with the EMD method, the EEMD method resolves the mode mixing problem and achieves better performance by adding white noise to the original signal (Z.Wu and N.E. Huang, 2004). For EEMD method, the first step is to produces an ensemble of datasets by adding the finite amplitude σ of Gaussian distribution white noise to the original data. The σ stands for standard deviation of white noise. Then EMD method is applied to each realization of datasets to get $IMF_i(t)$ with NE times repeatedly. The next step is that the expected \widehat{IMF}_j is obtained by averaging the respective components in each realization to compensate for the effect of the addition of Gaussian white noise.

$$\widehat{IMF}_j(t) = \frac{1}{NE} \sum_{i=1}^{NE} IMF_i(t) \quad (3)$$

where NE is the ensemble numbers. Finally, the result of the sifting procedure is that $S(t)$ will be decomposed into $\widehat{IMF}_j(t)$,

115 $j = 1, \dots, N$ and residual $r_N(t)$.

$$S(t) = \sum_{j=1}^N \widehat{IMF}_j(t) + r_N(t) \quad (4)$$

where σ is set between 0.05 to 0.2 and NE is set between 100 to 400. In this paper, we set σ and NE to 0.1 and 200 respectively.

2.3 EEMD-AF method

The EEMD method is equivalent to a sifting filter which sifts out each IMF component from signal $S(t)$ according to oscillations from fast to slow. The lower index IMF component mainly contains fast oscillations, meanwhile the higher index IMF component mainly contains slow oscillations. The baseline wander is expected to be captured by higher index IMFs. The simple removal of several higher index IMFs may introduce significant distortions of reconstructed signal.

Thus, the baseline wander is distributed over the desired components in several higher index IMFs. To suppress the baseline wander, this method introduces a group of adaptive low-pass filter to process the several higher index IMFs successively. The sum of the output of these filters is regarded as the reconstructed baseline estimate. Finally, the de-noised signal can be obtained by subtracting an estimated baseline from the noisy signal.

First of all, we suppose the signal $S(t)$ contained severe baseline wander. After processing by EEMD, $S(t)$ will be decomposed into IMFs which be referred to as $a_k(t)$.

$$S(t) = \sum_{k=1}^N a_k(t) \quad (5)$$

where N is the number of IMFs. Then, it is important to find out how much IMFs contribute to the baseline wander. Denote this number value as M . The $a_k(t)$ is processed from the higher to lower index by low-pass filter $h_k(t)$. The output of filter is $b_k(t)$.

$$b_k(t) = h_k(t) * a_k(t) \quad (6)$$

where $*$ denotes the convolution. The $h_k(t)$ is the Butterworth low-pass filter whose cut-off frequency is ω_k . As the IMF index decreases, fewer slow oscillations components, but more signal components are contained in each IMF. So, we design a group of adaptive low-pass filter whose cut-off frequency be decreased as IMF index decreases. In other words, the first processing of filter is that the last IMF, $a_N(t)$, convolved with the first low-pass filter whose cut-off frequency is $\omega_N(t)$. And the cut-off frequency decreased along with the k index filter decreased.

$$\omega_{k-1} = \omega_k * \alpha \quad (7)$$

where α is set between 0.1 to 0.99 and $k = N, \dots, 2, 1$. By this means the filter output $b_k(t)$ contained low-frequency components are extracted from each IMF. Because the algorithm has to be adaptive, the output can be used to determine value of M as the condition of the reconstructed signal. According to analysis of procedure above, the amplitude of the baseline should gradually decrease as the IMFs index decreases on filter output $b_k(t)$. As a result, to determine the value of M , we consider using evaluation coefficient function P_k as stopping criterion where the $\text{std}(b_k)$ stands for standard deviation b_k .

$$P_k = \frac{\text{flip}(\text{std}(b_k))}{\frac{1}{k-1} \sum_{i=1}^{k-1} \text{flip}(\text{std}(b_i))} \quad (8)$$

where $k = 1, 2, \dots, N$. The operator *flip* is the flipped function that the data rearrange in the opposite direction. The evaluation coefficient threshold δ is set whose value range from 0 to 0.1. If $P_k < \delta$, the value $M = N + 1 - k$. In this process, we set ω_N , α , δ to 10, 0.9 and 0.01 respectively. The sum of output of filtered IMFs whose index is from $M+1$ to N is regarded as the reconstructed baseline estimate.

$$\widehat{b}(t) = \sum_{k=M+1}^N b_k(t) \quad (9)$$

Finally, to obtain reconstructed de-noised signal, the baseline estimate is subtracted from the original signal.

$$\widehat{S}(t) = S(t) - \widehat{b}(t) \quad (10)$$

3 Simulation data analysis

3.1 Simulation data

155 In GREATEM system, the transmitter injects a bipolar square wave current into the ground, meanwhile the receiver and front-mounted coil were installed on an aircraft to response to the vertical component of the induced electromotive force in a horizontal layered earth model (Nabighian et al, 1988). Responded signals are related to the size and depth of underground conductor, the length and current of transmitter, the equivalent area of receiving coil, the horizontal offset, the flight altitude and so on. These parameters can be used to calculate the time domain response as clean signal in the horizontal layer earth model for simulation. In Fig. 1, the model parameters as follow: the length of transmitter line TX is 1000 m on the ground, the transmitter current is 10 A with 50% duty cycles at 25 Hz, the equivalent area of receiving coil RX is 1000 m², the horizontal offset is 50 m, the flight altitude is 35 m, the sample rate of receiver is 32k Hz. In this paper, we consider three-layer earth model where parameters are shown in Table 1. In the end, we calculated the corresponding time domain signal and the vertical response decay curve on a three-layer earth model.

160

165 Because of non-periodic and non-stationary characteristics of baseline wander, it is difficult to synthesize these noises from simulation on the computer. The simulated signal is obtained by superimposing the clean signal on the field baseline wander measured by the inertial navigation system. Fig. 2(a) is simulated noisy signal which is obtained by adding baseline wander to clean signal with the duration is 10 s. Fig. 2(b) is the field baseline wander noise which is measured by the inertial navigation system with the duration is 10 s.

170 3.2 Performance of the correction and analysis

In this paper, in order to quantitatively assess the de-noised quality between our method and other methods, we propose the signal-to-noise ratio (SNR) and mean square error (MSE) to evaluate the correctional methods in Equation 11 and 12, in which $S(n)$ is synthetic clean signal, $\widehat{S(n)}$ is de-noised signal, L is the number of samples. The higher the SNR, the better the correctional effect; the lower the MSE, the better the fitting result.

$$175 \quad \text{SNR} = 10\lg\left(\frac{\sum_{n=1}^L S^2(n)}{\sum_{n=1}^L (S(n) - \widehat{S(n)})^2}\right) \quad (11)$$

$$\text{MSE} = \frac{\sum_{n=1}^L (S(n) - \widehat{S(n)})^2}{L} \quad (12)$$

There are comparison of the SNR and MSE before and after correction using EEMD-AF, wavelet-based method with sym8 and level 10, and EEMD method with ignored higher index IMFs directly. Through the noisy signal of duration of 60 s is processed by three methods the correctional results are shown in Table 2, in which the term Noisy signal means simulated noisy signal before correction. The SNR value shows that the three methods have a remarkable improvement in signal quality. It is proved that EEMD-AF and wavelet-based method had better correctional performance than EEMD. Quantitatively, SNR of EEMD-AF method is significantly close to SNR achieved by the wavelet-based method. It is obvious that the EEMD-AF achieves correction performance as similar to the wavelet-based method.

180

For further analysis, the response decay curve is related to the conductivity of underground geological bodies in the data processing of GREATEM. Besides the SNR comparison above, the original data are used for stacking, averaging and extracting secondary field to build one by one test point along with the survey path. Then the number of time gates are 24 on per test point where the width of time gates increases approximately logarithmically.

To generate the anomaly curves profile image, we process the simulated noisy data and correctional data by stacking, averaging, extracting and gating. The anomaly curves profile generated from the clean signal responses is shown in Fig. 3(a), where the 24 paralleled line of time gates were represented along with the test point. And the Fig. 3(b) is anomaly curves profile generated from the noisy signal, where the fake anomaly from the Gate 14 to 24 is identified clearly due to baseline wander affected the horizontal layer model. From the Gate 20 to 24, they mixed each other. After the processing using the wavelet-based method, the anomaly curves profile is shown in Fig. 3(c), where the fake anomaly is not accurately represented and the curves are similar to parallel each other. Fig. 3(d) is the anomaly curves profile using the EEMD-AF method, it is pretty obvious that the paralleled curves between the gates are better than above method.

The comparison of SNR and MSE profile produced by the datasets on different method is illustrated in Fig. 4 along with the test point, where SNR and MSE of the noisy signal are marked as reference (black solid curve). In Fig. 4(a), the black solid curve shows that the stacking and averaging may produce the improved SNR for noisy signal. Quantitatively, the EEMD-AF and wavelet-based method yield SNR which is significantly higher than value achieved by the EEMD method. It is observed that there are fluctuations of SNR using wavelet-based method (blue solid curve) meanwhile there are stabilities of SNR using EEMD-AF method (red solid curve). And in Fig. 4(b), the MSE curves indicate the same conclusion. Results from the comparison of the figures also show that the EEMD-AF method significantly outperforms the wavelet-based for the suppression of non-stationary baseline wander.

4. Field data analysis

In October 2018, an field experimental GREATEM survey had been performed to detect infiltration water in the refuse landfill of Longquanyi District, Chengdu in China. The GREATEM system was developed by Chengdu University of Technology. The electrical source transmitter was fixed on the ground meanwhile the receiver system was mounted on the six rotor UAV. The survey area and flight paths of the receiver were shown in Fig. 5(b). The length of the transmitter line was 1100 m on the ground, the transmitter waveform was bipolar square wave and current was 20 A with 50% duty cycles at 5 Hz. The receiver system made use of 24-bit Analog-to-Digital Converter whose sample rate was 32k Hz and the equivalent area of the receiving coil was 1000 m². The transmitter line was set in the middle of flight paths and almost perpendicular to them. Each length of the flight path was 800 m and the intervals were 80 m each other. The flight speed of the UAV was 2.5 m/s and the height were 50 m from the ground.

The amplitude of the response will decrease with the transmitter–receiver offset increase. We choose measured data of part of flight path L4 for our processed, and the duration of 60 s of data is shown in Fig. 6(a). The baseline wander is observed on the

measured data significantly. And Fig. 6(b) is the correctional result from the EEMD-AF. By comparison of the signals before and after processing, the baseline wander is effectively suppressed by EEMD-AF method.

Besides the comparison of time domain data above, we produced anomaly curves profile image from the original measured data and the correctional data which is processed by the wavelet-based method and the EEMD-AF method respectively. The number of time gates is 18 and the widths are increase approximately logarithmically on per test point. Fig. 7(a) shows the anomaly curves profile generated from the measured raw data. The correctional data using the wavelet-based and EEMD-AF method are shown on Fig. 7(b) and (c) respectively. Based on the survey area for refuse landfill, the geological structure can be considered as layered earth, there may be partial regions where the infiltration water was leaked.

In Fig. 7(a), the higher amplitude of responded anomaly curves reflected at 220 m, 270 m and 300 m in the flight survey path. Therefore, the baseline wander exists in the original signal so as to affect exploration elevation and the anomalies result on inversion. It is obvious to observe the fake anomalies from the Gate 10 to 15 and the interference with each other from the Gate 16 to 18. In Fig. 7(b) and (c), after using two correction methods, the fake anomalies are suppressed on the Gate 10 to 15, and it is improved to interfere with each other from the Gate 16 to 18. In addition, the Fig.7(c) shows that there is no interference between the Gates. However, there is partial interference on the Gate 16 to 18 in Fig.7(b). Contrast with wavelet-based method, there is no interference between last three channels for datasets using EEMD-AF method on anomaly curves profile. For that the decay time of curves, the EEMD-AF method hold decay time 4.5 milliseconds more than wavelet-based method to improve the exploration elevation on the survey path. Comparison of Fig. 7(b) and (c), the results reveal that the performance of EEMD-AF method is significantly superior to the wavelet-based method to suppress baseline wander. In a word, the results confirm EEMD-AF method is an effective and practical correctional method.

5 Conclusion

Motion-induced noise was usually referred to as baseline wander which is an inevitable noise and always exists for GREATEM system. The noise caused by the receiving coil motion has its own characteristics such as low frequency, large amplitude, non-periodic and non-stationary. This phenomenon affects the accuracy of measurement severely, leading to the inferior exploration elevation and the fake anomalies result on inversion. Therefore, we proposed the improved EEMD-AF method for baseline wander correction. The noisy signal is decomposed into N-level IMF components and residual component by EEMD method, and the baseline wander is generally distributed over in several higher index IMFs, then a group of adaptive low-pass filter process these IMFs successively. The baseline estimate is reconstructed by the sum of these filter output. Finally, the de-noised signal can be obtained by subtracting an estimated baseline wander from the noisy signal.

First of all, through comparison of different de-noised method in this paper, the SNR and MSE results show that the de-noised performance of EEMD-AF method is significantly superior to the other methods. And the same conclusion can be reached from the anomaly curves profile image. Furthermore, in field data processed, the baseline wander is effectively suppressed by EEMD-AF and wavelet-based method. Because there is no interference between the last few Gates, the comparison of the

anomaly curves profile image reveals that EEMD-AF method is significantly better than the wavelet-based method. These results also indicate that the EEMD-AF method is a practical as well as effective method for the suppression of the baseline wander on GREATEM signal.

Data availability

In this paper, the data are not publicly accessible because funder terms require to kept confidential for the original geological data without cooperative licensing agreements.

Author contribution

First, Yuan L. and Song G. designed the method model and developed code. Second, the author Saimin Z. designed the field experiments and carried it out with Hu H. and Pengfei X. on survey area. Third, Yuan L. and Chunmei Y. performed the simulations and processed data. Finally, Yuan L. prepared the manuscript with contributions from all co-authors.

Competing interests

There are no competing interests in this paper. And the authors declare that they have no conflict of interest.

Acknowledgements

This study was carried out within the project ‘Research on fixed wing time domain airborne electromagnetic measurement technology system (2017YFC0601904)’ supported by the Institute of Geophysical and Geochemical Exploration, Chinese Academy of Geological Sciences. The authors thank the members of the project committee for their help.

- Abderrezak, B., Micheal, C., Pierre, K., Richard, S.: Sferics noise reduction in time-domain electromagnetic systems: application to MegaTEM II signal enhancement, *Explor. Geophys.*, 41, 225–239, doi:10.1071/EG09007, 2010.
- Buselli, G., Hwang, H.S., Pik, P.J.: AEM noise reduction with remote referencing, *Explor. Geophys.*, 29, 71–76, doi:10.1071/EG998071, 1998.
- 270 Blanco-Velasco M, Weng BW, Barner KE.: ECG signal denoising and baseline wander correction based on the empirical mode decomposition, *Comput. Biol. Med.*, 38, 1–13, doi:10.1016/j.combiomed.2007.06.003, 2008.
- Macnae, J.C., Lamontagne, Y., West, G.F.: Noise processing techniques for time-domain EM system, *Geophysics*, 49, 934–948, doi:10.1190/1.1826986, 1984.
- Fubo L., Jutao L., Lihua L.: Application of the EEMD method for distinction and suppression of motion-induced noise in grounded electrical source airborne TEM system, *J. Appl. Geophys.*, 139, 109–116, doi:10.1016/j.jappgeo.2017.02.013, 2017.
- 275 Lemire, D.: Baseline asymmetry, Tau projection, B-field estimation and automatic halfcycle rejection. Technical Report, THEM Geophysics Inc, 2001.
- Mogi, T., Tanaka, Y., Kusunoki, K., Morikawa, T., and Jomori, N.: Development of grounded electrical source airborne transient EM(GREATEM), *Explor. Geophys.*, 29, 61–64, doi:10.1071/EG998061, 1998.
- 280 Nabighian, M.N.: Electromagnetic methods in applied geophysics, Volume 1: Theory. Soc. Explor. Geophys., doi:10.1007/bf01452955, 1988.
- N.E. Huang, Z. Shen, S.R. Long, M.C. Wu, H.H. Shin, Q. Zheng, N.C. Yen, C.C. Tung and H.H. Liu: The Empirical Mode Decomposition and the Hilbert spectrum for nonlinear and non-stationary time series analysis, *Proc. Royal Soc. London A*, vol. 454, 903–995, doi:10.1098/rspa.1998.0193, 1998.
- 285 P. Flandrin, P. Goncalves, G. Rilling: Detrending and denoising with empirical mode decomposition, 12th European Signal Processing Conference, Vienna, Austria, September 2004.
- Smith, R. S., Annan, A. P., and McGowan, P. D.: A comparison of data from airborne, semi-airborne and ground electromagnetic systems, *Geophysics*, 66, 1379–1385, doi:10.1190/1.1487084, 2001.
- Wang, Y., Ji, Y.J., Li, S.Y., et al.: A wavelet-based baseline drift correction method for grounded electrical source airborne transient electromagnetic signals, *Explor. Geophys.*, 44, 229–237, doi:10.1071/EG12078, 2013.
- 290 Z. Wu, N.E. Huang.: Ensemble empirical mode decomposition: a noise-assisted data analysis method, *Adv. Adapt. Data Anal.*, 1, 1–41, doi:10.1142/S1793536909000047, 2009.
- Z. Wu, N.E. Huang.: A study of the characteristics of white noise using the empirical mode decomposition method, *Proc. R. Soc. A* 460 (2046), 1597–1611, doi:10.1098/rspa.2003.1221, 2004.

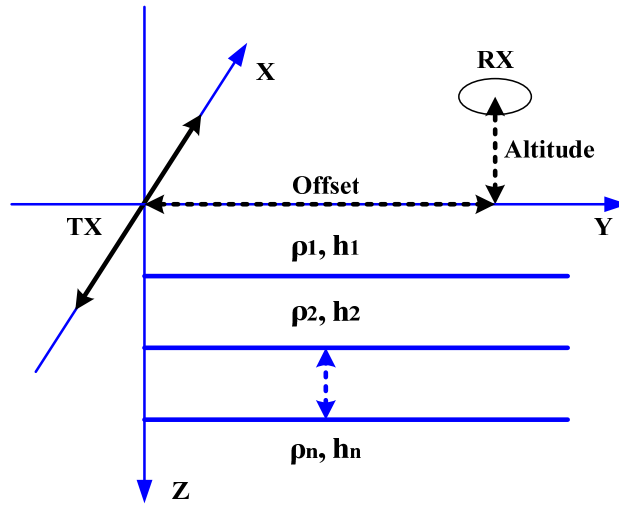


Figure 1: GREATEM model based on three-layer earth model. The TX is the transmitter line on the ground and the line length is 1000 m, the transmitter current is 10 A and frequency is 25 Hz. The RX is receiving coil and the equivalent area is 1000 m², the offset is 50 m, the flight altitude is 35 m, the sample rate of receiver is 32k Hz. The other model parameters are shown in Table 1.

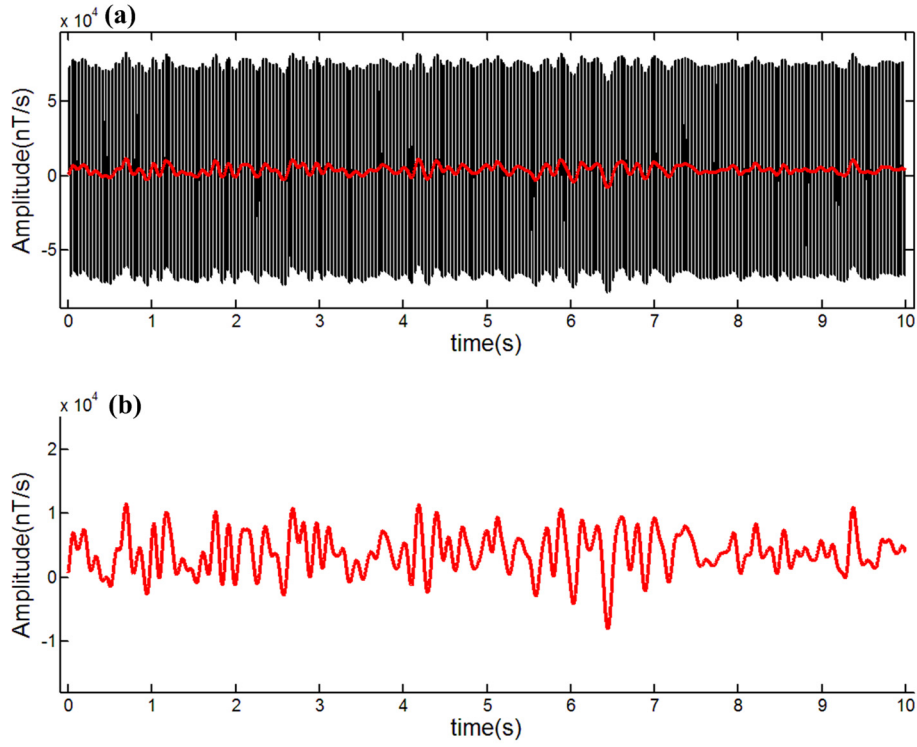


Figure 2: The simulated noisy signal and baseline wander signal whose duration is 10 s. (a) The simulated noisy signals; (b) the field baseline wander measured by the inertial navigation system.

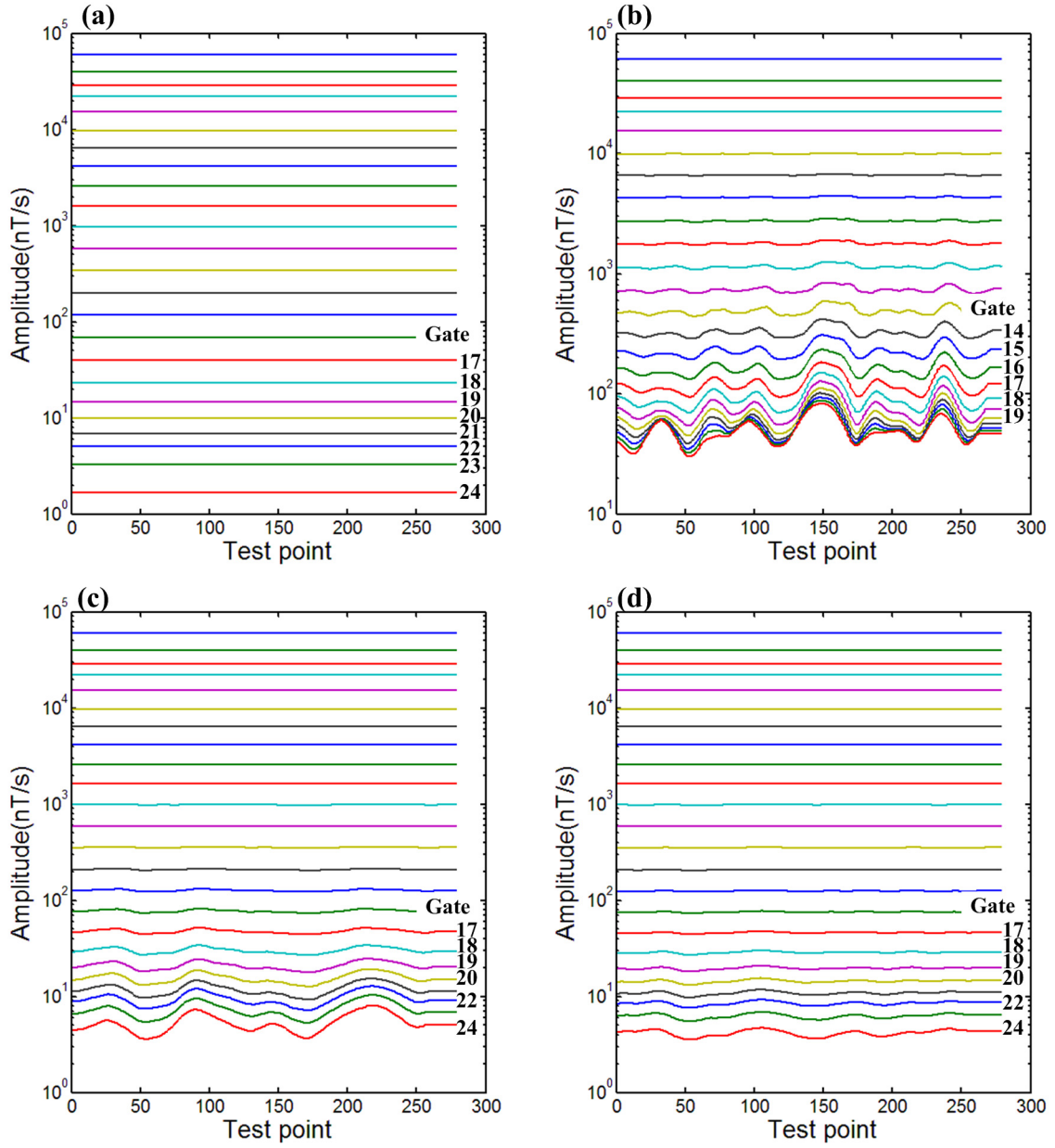


Figure 3: Anomaly curves profile image generated from different processed datasets. The duration of raw data is 60 s and the stacking interval is 0.2 s therefore the number of Test points is 300. (a) The clean signal from the theoretical model; (b) the noisy signal containing baseline wander; (c) the correctional signal using wavelet-based method; (d) the correctional signal using EEMD-AF method. The label Gate marked in each figure represents the number of time gates from 1 to 24. Every specific number of time gate means different time width which increased logarithmically.

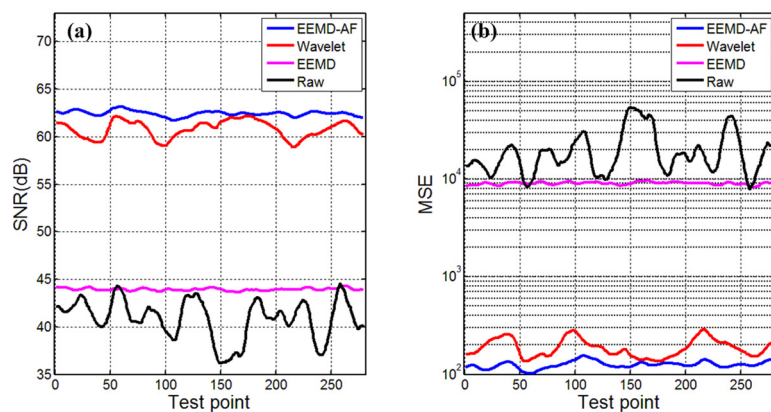


Figure 4: Comparison of SNR and MSE profile produced by the datasets on different methods along with test point. (a) The contrast of SNR on different datasets; (b) the contrast of MSE on different datasets.

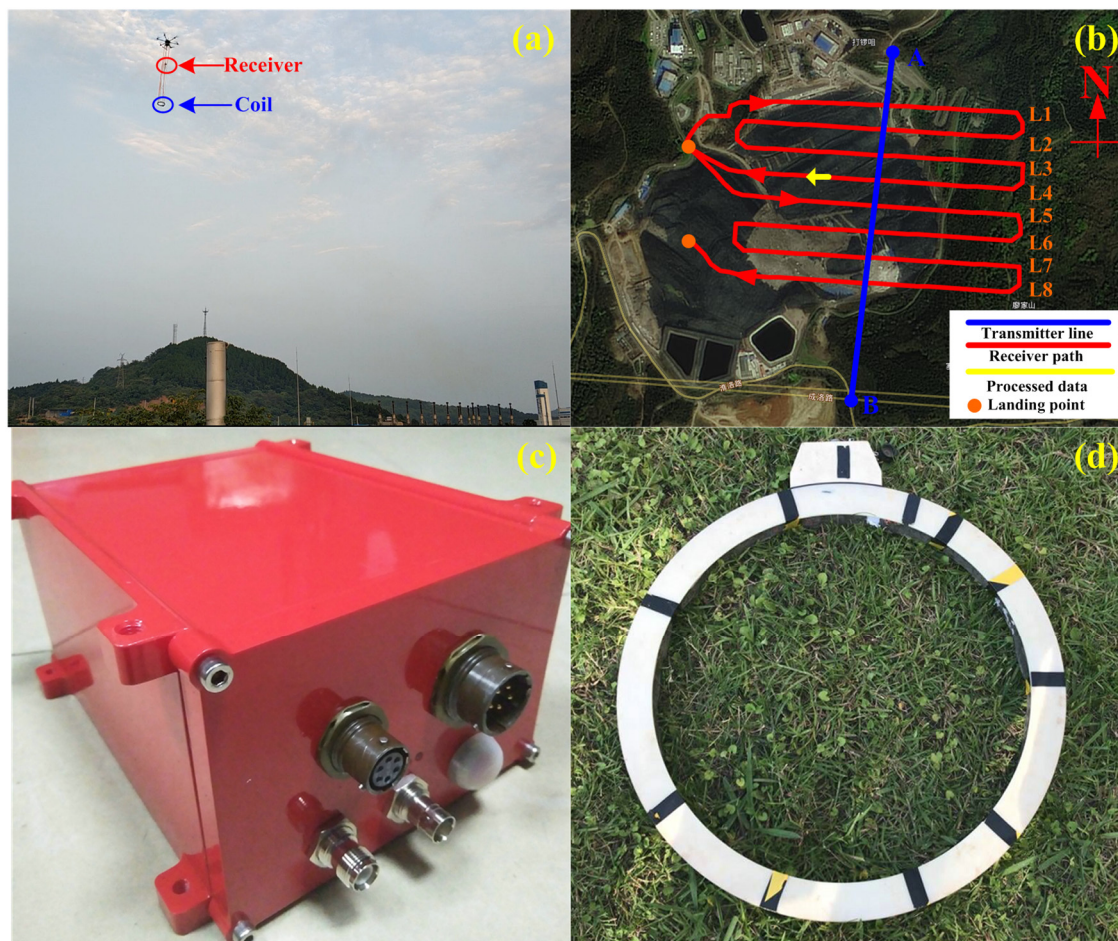


Figure 5: The survey area and flight paths on the refuse landfill of Longquanyi District, Chengdu in China. (a) The receiver system is mounted on UAV along with the paths; (b) the blue line was the transmitter source and the red curves were the survey paths of the receiver, the lines of L1 through L8 represent different paths and the orange dots represent the landing point for UAV; (c) the receiver system is mounted on UAV along with the paths; (d) the receiver system is mounted on UAV along with the paths.

receiver instruments; (d) the receiving coil with diameter of 50 cm. The flight heading was from east to west on the L4 path. The data of part of L4 (yellow arrow solid line) will be processed and the duration was 60 s. The satellite image embedded in figure (b) came from <https://map.tianditu.gov.cn/> built by the National Geomatics Center of China.

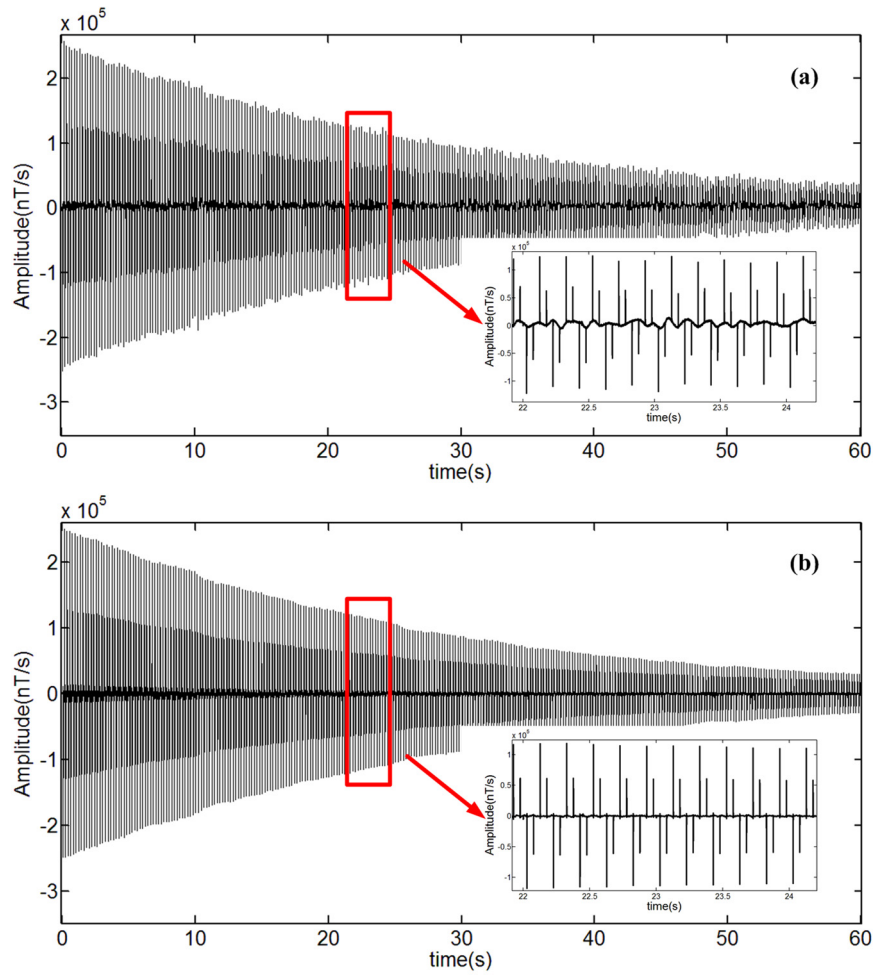


Figure 6: The field data whose duration is 60 s containing baseline wander and correctional data filtered by the EEMD-AF method. (a) The field data measured by receiver instruments; (b) the correctional data using the EEMD-AF method. The data of 22 s to 24 s is magnified and shown at the lower right of each figure.

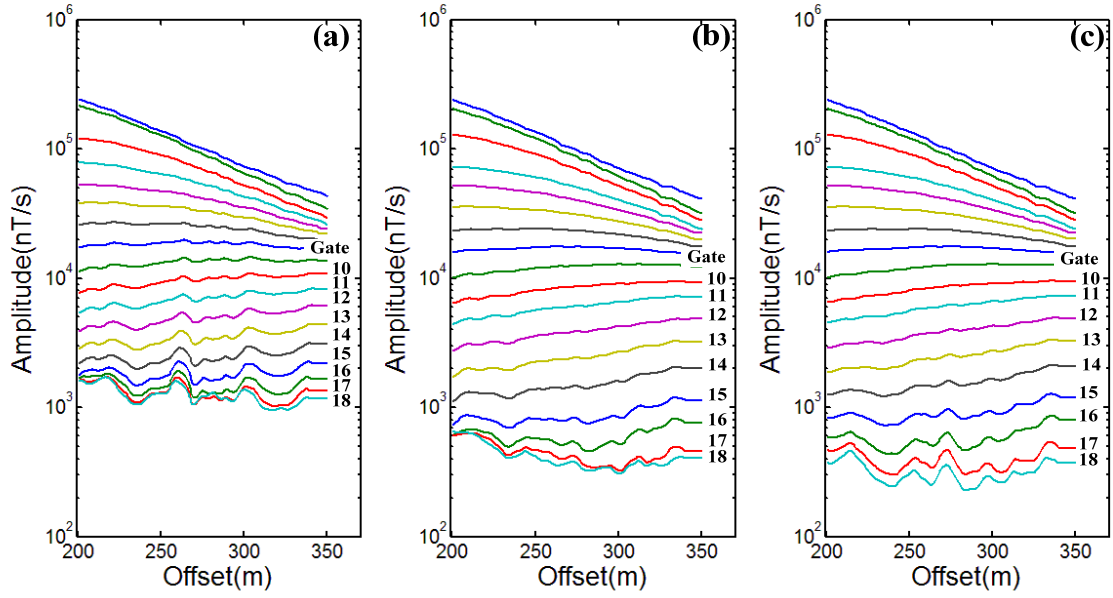


Figure 7: Anomaly curves profile image generated from field data on different methods. (a) The profile of raw data; (b) the profile of data using wavelet-based method; (c) the profile of data using EEMD-AF method. Because the duration of raw data was 60 s and the flight speed of the UAV was 2.5 m/s, the offset distance was 150 m.

Table 1: Parameters of the three-layer earth model

Parameter	Resistivity ρ_n (Ω m)	Thickness h_n (m)
1st	150	100
2nd	30	100
3th	300	

Table 2 Correctional result comparison of SNR of different methods

Method	SNR(dB)
Noisy signal	5.0810
EEMD-AF	48.1462
EEMD	35.1025
Wavelet-based	48.2513